Investigation of a bicyclo[1.1.1]pentane as a phenyl replacement within an $LpPLA_2$ inhibitor

Nicholas D. Measom[a,b], Kenneth D. Down[a], David J. Hirst[a], Craig Jamieson[b], Eric S. Manas[c], Vipulkumar K. Patel[a], Don O. Somers[a]

a – GlaxoSmithKline, Medicines Research Centre, Gunnels Wood Road, Stevenage, Hertfordshire, SG1 2NY, UK

b – Department of Pure and Applied Chemistry, University of Strathclyde, Thomas Graham Building, 295 Cathedral Street, Glasgow, G1 1XL, UK

c – GlaxoSmithKline, 1250 S. Collegeville Road, Collegeville, Pennsylvania, 19426-0989, USA

ABSTRACT: We describe the incorporation of a bicyclo[1.1.1]pentane moiety within two known $LpPLA_2$ inhibitors to act as bioisosteric phenyl replacements. An efficient synthesis to the target compounds was enabled with a dichlorocarbene insertion into a bicyclo[1.1.0]butane system being the key transformation. Potency, physicochemical and X-ray crystallographic data were obtained to compare the known inhibitors to their bioisosteric counterparts, which showed the isostere was well tolerated and positively impacted on the physicochemical profile.

Keywords: $LpPLA_2$, bicyclo[1.1.1]pentane, bioisostere, darapladib, cardiovascular disease, physicochemical.

Lipoprotein-associated phospholipase A2 ($LpPLA_2$) or platelet-activating factor acetylhydrolase (PAF-AH) has been extensively studied as a potential therapeutic target for the treatment of atherosclerosis[1–6] and more recently in other diseases where vascular inflammation may play a role e.g. diabetic macular edema and Alzheimer's disease.[7,8] A range of epidemiological and genetic evidence suggests that increased $LpPLA_2$ concentration increases the risk of myocardial infarction (MI), ischemic stroke and cardiac death in patients with stable cardiovascular disease (CVD).[1,9–26] With considerable support for the hypothesis that $LpPLA_2$ is associated with atherosclerosis, a range of inhibitors have been developed, with darapladib, **1**[27–29] and rilapladib, **2**[30] being well studied examples as both compounds have entered clinical trials (Figure 1).

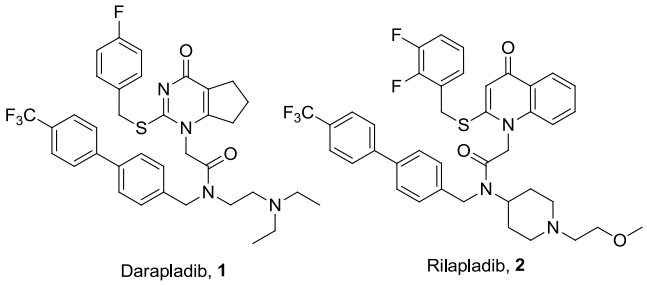

Figure 1 – Darapladib and rilapladib structures

Compound **1** (Figure 1) shows excellent potency against $LpPLA_2$ in *in vitro* assays with a pIC_{50} of 10.2.[28] It is highly lipophilic ($ChromLogD_{7.4}$: 6.3) although does however, have good artificial membrane permeability (AMP) of 230 nm/s. *In vivo* studies have consistently shown inhibition of the hydrolysis of $LpPLA_2$ substrates in rats, dogs, rabbits and pigs.[28] The *in vivo* effects of **1** include reduced content of lyso-phosphatidylcholines (lyso-PCs) within atherosclerotic lesions, which are pro-inflammatory mediators.[31] Both compounds **1** and **2**(Figure 1) bind to $LpPLA_2$ in a similar manner with the cyclic amide/ketone mimicking the ester functionality of the enzyme substrates within the oxyanion hole.[32,33] This blocks the active site where a Ser273, His351 and Asp296 form the catalytic triad and the backbone amide NHs of a Leu153 and Phe274 help to bind the substrate (Figure 5). The remaining functionality occupies lipophilic pockets adjacent to the active site. Compound **2** similarly displays excellent $LpPLA_2$ potency in *in vitro* assays. Both inhibitors, however, exhibit sub-optimal physicochemical profiles. They have high molecular weights, low aqueous solubility and high property forecast indices (PFI); a risk indicator of developability.[34] Improvement of the physicochemical properties of these compounds is therefore attractive. Methods of achieving this include: introduction of polar functionality; removal of lipophilic groups or replacement of sub-optimal groups, such as aromatic rings with suitable bioisosteres, all of which were postulated to positively impact parameters such as PFI.[34]

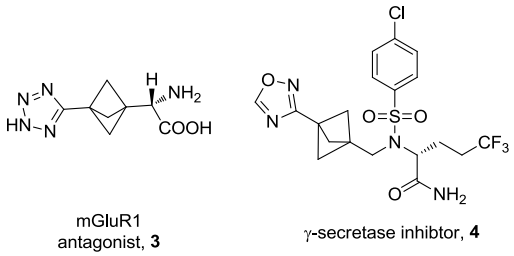

Figure 2 – Drug compounds with [1.1.1]bicyclopentane moiety

Scheme 1 - Synthesis of key intermediate 13

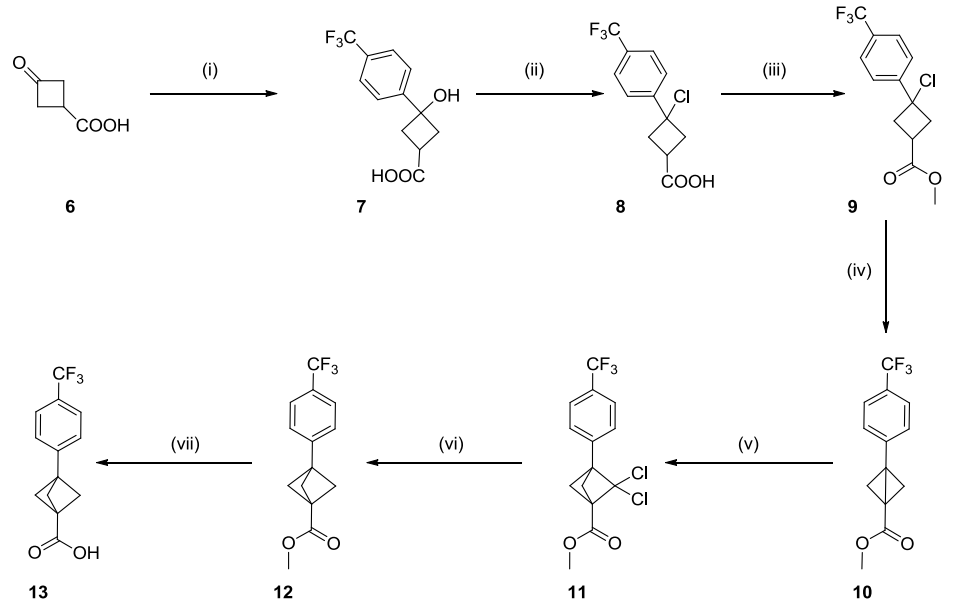

Reagents and conditions: (i) 4-bromotrifluorotoluene, nBuLi, THF, -78 °C to rt, 77%; (ii) conc. HCl, PhMe, rt, sonication, 75%; (iii) HCl, MeOH, 1,4-dioxane, rt, quant.; (iv) NaH, THF, rt, 98%; (v) sodium trichloroacetate, tetrachloroethylene, diglyme, 120 °C to 140 °C, 38%; (vi) tris(trimethylsilyl)silane, 1,1'-azobis(cyclohexanecarbonitrile), PhMe, 110 °C, 74%; (vii) LiOH, 1,4-doxane, rt, 95%.

In this regard we targeted replacement of aromatic rings with saturated isosteres and became interested in the bicyclo[1.1.1]pentane system. There are a paucity of examples of the use of this template as a phenyl bioisostere[35–37] including an mGluR1 receptor antagonist **3**[38,39] and a γ-secretase inhibitor **4** (Figure 2).[40] This is possibly due to the lack of tractable routes to the desired analogues. Despite this, we reasoned it could serve as a useful isostere of the aryl unit in the darapladib chemotype (Figure 3).

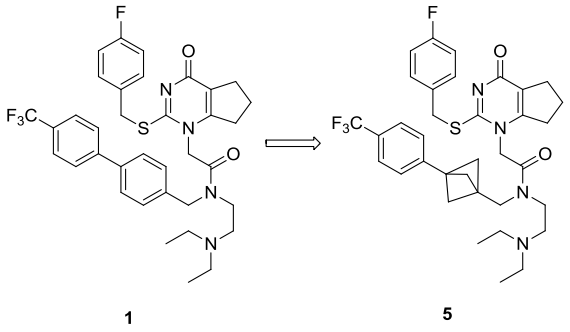

Figure 3 – Potential isosteric replacement for darapladib

Accordingly, in this letter we illustrate the successful incorporation of the bicyclo[1.1.1]pentane into both the darapladib and rilapladib structures. The crystal structure of darapladib bound to $LpPLA_2$, solved in-house and comparable to the structure recently published,[33] indicates the internal aromatic of the bi-aryl system acts as a spacer, to allow access to a lipophilic pocket occupied by the trifluoromethylphenyl group. Modeling of the bicyclo[1.1.1]pentane moiety within $LpPLA_2$, and comparison with the X-ray structure of darapladib, confirmed its potential viability as a replacement linker (Figure 4). It was envisaged that disrupting the planarity of the biaryl system would improve the physicochemical profile.

There are only two previously reported syntheses of the bicyclo[1.1.1]pentane moiety.[41,42] These include utilizing a propellane as the key intermediate followed by a photochemical acetylation.[43] Alternatively, addition of a carbene derivative to a bicyclo[1.1.0]butane followed by dechlorination can be employed.[42] The latter was deemed more suitable for large scale chemistry and was therefore exploited in these syntheses.

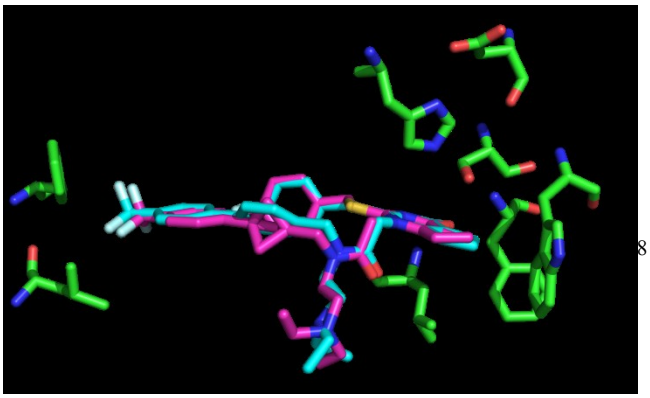

Figure 4 – X-ray crystal structure of darapladib (blue) in $LpPLA_2$ overlaid with modeled bioisosteric replacement (magenta)

The synthesis of key intermediate **13** commenced with an organometallic addition into the commercially available ketone **6** to furnish **7** as approximately a 2:1 ratio of diastereomers in good yield. Alcohol **7** was converted to the chloride, and subsequent esterification and cyclisation gave intermediate **10** with all steps proceeding in good to excellent yield.[44] The bicyclo[1.1.0]butane derivative **10** was treated with a dichlorocarbene[42] to generate **11** in a yield comparable with literature. Alternative carbene additions, including a Simmons Smith reagent, were investigated, however, these all proved unsuccessful. In a modification to the established process dechlorination of

the ring system was achieved utilizing a tin hydride replacement; tris(trimethylsilyl)silane (TTMSS).[39,45] Dechlorination proceeded smoothly and subsequent ester hydrolysis furnished the key carboxylic acid intermediate **13** in excellent yield (Scheme 1).

Intermediate **13** was then used in the synthesis of both $LpPLA_2$ analogues. Amide coupling of **13** with commercially available amine **14** followed by reduction of the resulting amide **15** furnished intermediate **16** in good yield. Subsequent amide coupling of **16** with fragment **17**[28] secured the darapladib analogue **5** (Scheme 2).

Scheme 2 – Synthesis of bioisosteric darapladib analogue 5

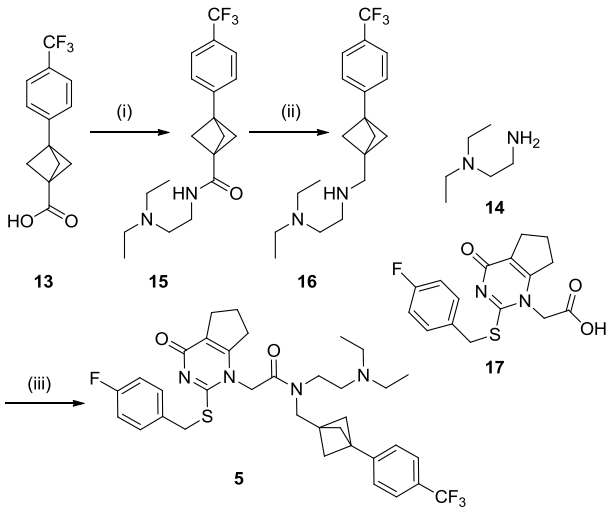

Reagents and Conditions: (i) **14**, T3P, Et_3N, EtOAc, rt, 99%; (ii) $LiAlH_4$, THF, rt, 56%; (iii) **17**, T3p, Et_3N, rt, 60%.

Analogue **22** was synthesized in a similar fashion starting with an amide coupling of **13** with commercially available amine **18**. Subsequent reduction[46] of the resulting amide **19** to give intermediate **20**, followed by amide coupling with fragment **21**[47] produced the desired compound **22** in moderate yield (Scheme 3).

Scheme 3 – Synthesis of bioisosteric rilapladib analogue 22

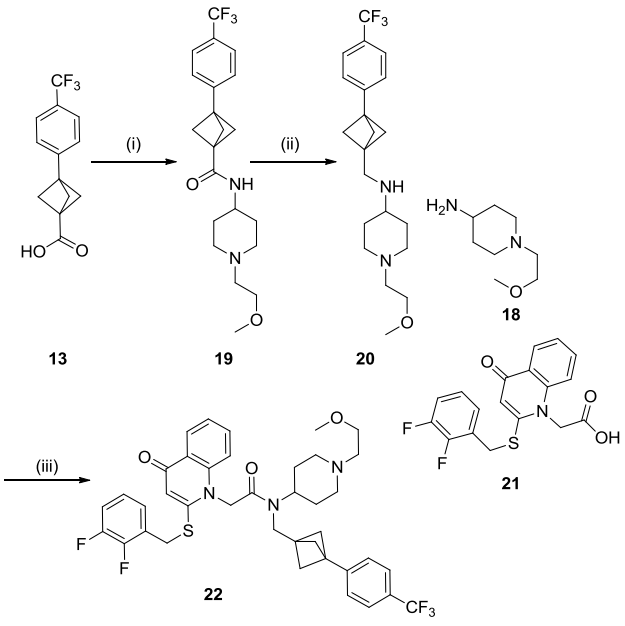

Reagents and conditions: (i) **18**, T3P, Et_3N, CH_2Cl_2, rt, 74%; (ii) $[Ir(COE)_2Cl]_2$, Et_2SiH_2, CH_2Cl_2, rt, 59%; (iii) **21**m T3P, Et_3N, CH_2Cl_2, rt, 53%.

With target compound **5** in hand, a comparison of its enzyme potency and physicochemical properties with that of darapladib was undertaken. Data collected included $LpPLA_2$ potency, solubility, $ChromLogD_{7.4}$ (and associated PFI[34]), as well as AMP binding. Analogue **5** maintains high potency compared to that of its parent **1** with a pIC_{50} of 9.4 (**1** pIC_{50} = 10.2). This suggested that the bioisosteric moiety was tolerated within the enzyme. In order to compare the binding mode of the bioisosteric analogue **5** with darapladib, an X-ray crystal structure of **5** in the $LpPLA_2$ protein was generated.[48] The structure, solved at ~1.9 Å resolution, revealed a similar binding mode for both molecules (Figure 5), which is in agreement with the initial molecular modeling (Figure 4). The overlay of the two structures reveals that the bicyclo[1.1.1]pentane moiety slightly precludes the adjacent tri-fluorophenyl moiety extending as far towards Leu121 and Phe125, although these residues move slightly towards the inhibitor to fill the void. This sub-optimal occupancy of the pocket could be an important factor in the slight drop-off in potency. Furthermore, the moiety has no effect on the key interactions within the oxyanion hole; retaining the carbonyl to backbone amide NH bonds with Leu153 and Phe274 residues and subsequently blocking the catalytic triad.

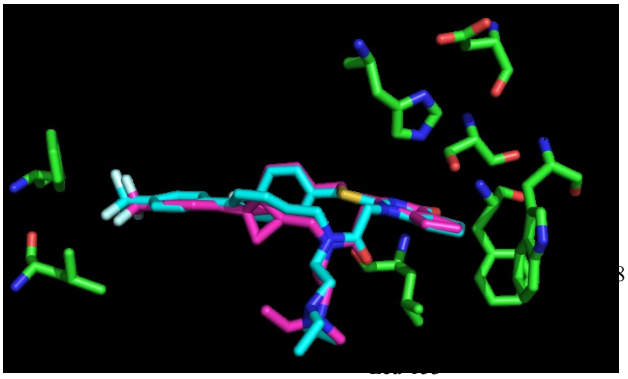

Figure 5 – X-ray crystal structure overlays of bound darapladib (blue) and analogue 5 (magenta) in $LpPLA_2$

With the binding mode of both progenitor compound **2** and analogue **5** confirmed, a physicochemical comparison of both was conducted (Table 1).

Table 1 - Summary of physicochemical data

	1	**5**	**2**	**22**
pIC_{50}	10.2	9.4	NT*	9.6[52]
CLND (µM)	8	74	<1	32
FaSSIF (µg/mL)	399	>1000	203	635
AMP (nm/s)[49]	230	705	NT*	NT*
ChromLogD	6.3	7.0	6.74	7.06
PFI	10.3	10.0	11.74	11.06

*NT = Not tested

Analogue **5** showed an improved permeability of 705 nm/s from 230 nm/s[49] and a 9-fold increase in kinetic solubility over darapladib (74 vs. 8 μM respectively). However, this was accompanied by an undesired increase in lipophilicity as determined by measured $ChromLogD_{7.4}$ from 6.3 to 7.0. Calculation of Property Forecast Index, which is a summation of $ChromLogD_{7.4}$ and number of aromatic rings[34] consequently indicated that the compounds **1** and **5** have equivalent PFIs due to the removal of one aromatic ring. Thermodynamic fasted state simulated intestinal fluid (FaSSIF) solubility was also obtained with analogue **5** exhibiting an approximately 3-fold improvement (>1000 μg/mL compared to 399 μg/mL). This data is echoed by the comparison of **2** and **22**, with **22** displaying improved solubility at pH 7.4 in both kinetic and thermodynamic measures as well as equivalent PFIs. Additionally, low clearance was observed for both **5** and **22** in a human liver microsomal assay, 1.2228 mL/min/g and 0.7607 mL/min/g respectively. These data lend weight to the hypothesis that disrupting molecular planarity[40,50,51] and reducing aromatic ring count[34] can be beneficial to solubility and the overall pharmacokinetic profile.

In summary, the incorporation of the bioisoteric bicyclo[1.1.1]pentane replacement, within $LpPLA_2$ analogues **5** and **22,** respectively has been enabled through a challenging synthesis. High potency was maintained for **5** and the binding mode was confirmed by X-ray crystallography.[48] The [1.1.1]bicyclopentane moiety imparts improved physicochemical properties compared to the known inhibitor. This confirms the utility of this group as a phenyl bioisostere in the context of $LpPLA_2$ inhibition.

Supporting Information

Acknowledgements

N.D.M. is grateful to GlaxoSmithKline R&D, Stevenage for Ph.D. studentship funding. We would also like to thank Sean Lynn for his help with the NMR assignments; Florent Potvain, Pascal Grondin and Marie-Hélène Fouchet for running of the Lp-PLA_2 assay; the Physicochemical Analysis Team; and Storm Hart and Thomas Clohessy for their intellectual input.

References

(1) Rosenson, R. S.; Stafforini, D. M. Modulation of Oxidative Stress, Inflammation, and Atherosclerosis by Lipoprotein-Associated Phospholipase A2. *J. Lipid Res.* **2012**, *53* (9), 1767–1782.

(2) Burke, J. E.; Dennis, E. A. Phospholipase A2 Biochemistry. *Cardiovasc Drugs Ther.* **2009**, *23* (1), 49–71.

(3) Schaloske, R. H.; Dennis, E. A. The Phospholipase A2 Superfamily and Its Group Numbering System. *Biochim. Biophys. Acta - Mol. Cell Biol. Lipids* **2006**, *1761* (11), 1246–1259.

(4) Stremler, K. E.; Stafforini, D. M.; Prescott, S. M.; McIntyre, T. M. Human Plasma Platelet-Activating Factor Acetylhydrolase. Oxidatively Fragmented Phospholipids as Substrates. *J. Biol. Chem.* **1991**, *266* (17), 11095–11103.

(5) Steinbrecher, U. P.; Pritchard, P. H. Hydrolysis of Phosphatidylcholine during LDL Oxidation Is Mediated by Platelet-Activating Factor Acetylhydrolase. *J. Lipid Res.* **1989**, *30* (3), 305–315.

(6) Marathe, G. K.; Harrison, K. A.; Murphy, R. C.; Prescott, S. M.; Zimmerman, G. A.; McIntyre, T. M. Bioactive Phospholipid Oxidation Products. *Free Radic. Biol. Med.* **2000**, *28* (12), 1762–1770.

(7) Staurenghi, G.; Ye, L.; Magee, M. H.; Danis, R. P.; Wurzelmann, J.; Adamson, P.; McLaughlin, M. M. Darapladib, a Lipoprotein-Associated Phospholipase A2 Inhibitor, in Diabetic Macular Edema: A 3-Month Placebo-Controlled Study. *Ophthalmology* **2015**, *122* (5), 990–996.

(8) Maher-Edwards, G.; De'Ath, J.; Barnett, C.; Lavrov, A.; Lockhart, A. A 24-Week Study to Evaluate the Effect of Rilapladib on Cognition and CSF Markers of Alzheimer's Disease. *Alzheimer's Dement.* **2014**, *10* (June), 301–302.

(9) White, H. Editorial: Why Inhibition of Lipoprotein-Associated Phospholipase A2 Has the Potential to Improve Patient Outcomes. *Curr. Opin. Cardiol.* **2010**, *25* (4), 299–301.

(10) The LpPLA2 Studies Collaboration. Lipoprotein-Associated Phospholipase A2 and Risk of Coronary Disease, Stroke, and Mortality: Collaborative Analysis of 32 Prospective Studies. *Lancet* **2010**, *375* (9725), 1536–1544.

(11) Kiechl, S.; Willeit, J.; Mayr, M.; Viehweider, B.; Oberhollenzer, M.; Kronenberg, F.; Wiedermann, C. J.; Oberthaler, S.; Xu, Q.; Witztum, J. L.; Tsimikas, S. Oxidized Phospholipids, Lipoprotein(a), Lipoprotein-Associated Phospholipase A2 Activity, and 10-Year Cardiovascular Outcomes: Prospective Results From the Bruneck Study. *Arterioscler. Thromb. Vasc. Biol.* **2007**, *27* (8), 1788–1795.

(12) Tsimikas, S.; Mallat, Z.; Talmud, P. J.; Kastelein, J. J. P.; Wareham, N. J.; Sandhu, M. S.; Miller, E. R.; Benessiano, J.; Tedgui, A.; Witztum, J. L.; Khaw, K.-T.; Boekholdt, S. M. Oxidation-Specific Biomarkers, Lipoprotein(a), and Risk of Fatal and Nonfatal Coronary Events. *J. Am. Coll. Cardiol.* **2010**, *56* (12), 946–955.

(13) Ryu, S. K.; Mallat, Z.; Benessiano, J.; Tedgui, A.; Olsson, A. G.; Bao, W.; Schwartz, G. G.; Tsimikas, S. Phospholipase A2 Enzymes, High-Dose Atorvastatin, and Prediction of Ischemic Events After Acute Coronary Syndromes. *Circulation* **2012**, *125* (6), 757–766.

(14) Mallat, Z.; Lambeau, G.; Tedgui, a. Lipoprotein-Associated and Secreted Phospholipases A2 in Cardiovascular Disease: Roles as Biological Effectors and Biomarkers. *Circulation* **2010**, *122* (21), 2183–2200.

(15) Koenig, W. Lipoprotein-Associated Phospholipase A2 Predicts Future Cardiovascular Events in Patients With Coronary Heart Disease Independently of Traditional Risk Factors, Markers of Inflammation, Renal Function, and Hemodynamic Stress. *Arterioscler. Thromb. Vasc. Biol.* **2006**, *26* (7), 1586–1593.

(16) Sabatine, M. S.; Morrow, D. A.; O'Donoghue, M.; Jablonksi, K. A.; Rice, M. M.; Solomon, S.; Rosenberg, Y.; Domanski, M. J.; Hsia, J. Prognostic Utility of Lipoprotein-Associated Phospholipase A2 for Cardiovascular Outcomes in Patients With Stable Coronary Artery Disease. *Arterioscler. Thromb. Vasc. Biol.* **2007**, *27* (11), 2463–2469.

(17) Brilakis, E. S. Association of Lipoprotein-Associated Phospholipase A2 Levels with Coronary Artery Disease Risk Factors, Angiographic Coronary Artery Disease, and Major Adverse Events at Follow-Up. *Eur. Heart J.* **2004**, *26* (2), 137–144.

(18) Stafforini, D. M.; Satoh, K.; Atkinson, D. L.; Tjoelker, L. W.; Eberhardt, C.; Yoshida, H.; Imaizumi, T.; Takamatsu, S.; Zimmerman, G. A.; McIntyre, T. M.; Gray, P. W.; Prescott, S. M. Platelet-Activating Factor Acetylhydrolase Deficiency. A Missense Mutation near the Active Site of an Anti-Inflammatory Phospholipase. *J. Clin. Invest.* **1996**, *97* (12), 2784–2791.

(19) Miwa, M.; Miyake, T.; Yamanaka, T.; Sugatani, J.; Suzuki, Y.; Sakata, S.; Araki, Y.; Matsumoto, M. Characterization of Serum Platelet-Activating Factor (PAF) Acetylhydrolase. Correlation between Deficiency of Serum PAF Acetylhydrolase and Respiratory Symptoms in Asthmatic Children. *J. Clin. Invest.* **1988**, *82* (6), 1983–1991.

(20) Yamada, Y.; Yoshida, H.; Ichihara, S.; Imaizumi, T.; Satoh, K.; Yokota, M. Correlations between Plasma Platelet-Activating Factor Acetylhydrolase (PAF-AH) Activity and PAF-AH Genotype, Age, and Atherosclerosis in a Japanese Population. *Atherosclerosis* **2000**, *150* (1), 209–216.

(21) Yamada, Y.; Izawa, H.; Ichihara, S.; Takatsu, F.; Ishihara, H.; Hirayama, H.; Sone, T.; Tanaka, M.; Yokota, M. Prediction of the Risk of Myocardial Infarction from Polymorphisms in Candidate Genes. *N. Engl. J. Med.* **2002**, *347* (24), 1916–1923.

(22) Yamada, Y.; Ichihara, S.; Fujimura, T.; Yokota, M. Identification of the G994--> T Missense in Exon 9 of the Plasma Platelet-Activating Factor Acetylhydrolase Gene as an Independent Risk Factor for Coronary Artery Disease in Japanese Men. *Metabolism.* **1998**, *47* (2), 177–181.

(23) Unno, N.; Nakamura, T.; Kaneko, H.; Uchiyama, T.; Yamamoto, N.; Sugatani, J.; Miwa, M.; Nakamura, S. Plasma Platelet-Activating Factor Acetylhydrolase Deficiency Is Associated with Atherosclerotic Occlusive Disease in Japan. *J. Vasc. Surg.* **2000**, *32* (2), 263–267.

(24) Hiramoto, M.; Yoshida, H.; Imaizumi, T.; Yoshimizu, N.; Satoh, K. A Mutation in Plasma Platelet-Activating Factor Acetylhydrolase (Val279->Phe) Is a Genetic Risk Factor for Stroke. *Stroke* **1997**, *28* (12), 2417–2420.

(25) Jang, Y.; Waterworth, D.; Lee, J.-E.; Song, K.; Kim, S.; Kim, H.-S.; Park, K. W.; Cho, H.-J.; Oh, I.-Y.; Park, J. E.; Lee, B.-S.; Ku, H. J.; Shin, D.-J.; Lee, J. H.; Jee, S. H.; Han, B.-G.; Jang, H.-Y.; Cho, E.-Y.; Vallance, P.; Whittaker, J.; Cardon, L.; Mooser, V. Carriage of the V279F Null Allele within the Gene Encoding Lp-PLA2 Is Protective from Coronary Artery Disease in South Korean Males. *PLoS One* **2011**, *6* (4), 18208–18214.

(26) Jang, Y.; Kim, O. Y.; Koh, S. J.; Chae, J. S.; Ko, Y. G.; Kim, J. Y.; Cho, H.; Jeong, T.-S.; Lee, W. S.; Ordovas, J. M.; Lee, J. H. The Val279Phe Variant of the Lipoprotein-Associated Phospholipase A2 Gene Is Associated with Catalytic Activities and Cardiovascular Disease in Korean Men. *J. Clin. Endocrinol. Metab.* **2006**, *91* (9), 3521–3527.

(27) The Stability Investigators. Darapladib for Preventing Ischemic Events in Stable Coronary Heart Disease. *N. Engl. J. Med.* **2014**, *370* (18), 1702–1711.

(28) Blackie, J. A.; Bloomer, J. C.; Brown, M. J. B.; Cheng, H.-Y.; Hammond, B.; Hickey, D. M. B.; Ife, R. J.; Leach, C. A.; Lewis, V. A.; Macphee, C. H.; Milliner, K. J.; Moores, K. E.; Pinto, I. L.; Smith, S. A.; Stansfield, I. G.; Stanway, S. J.; Taylor, M. A.; Theobald, C. J. The Identification of Clinical Candidate SB-480848: A Potent Inhibitor of Lipoprotein-Associated Phospholipase A2. *Bioorg. Med. Chem. Lett.* **2003**, *13* (6), 1067–1070.

(29) O'Donoghue, M. L.; Braunwald, E.; White, H. D.; Steen, D. P.; Lukas, M. A.; Tarka, E.; Steg, P. G.; Hochman, J. S.; Bode, C.; Maggioni, A. P.; Im, K.; Shannon, J. B.; Davies, R. Y.; Murphy, S. A.; Crugnale, S. E.; Wiviott, S. D.; Bonaca, M. P.; Watson, D. F.; Weaver, W. D.; Serruys, P. W.; Cannon, C. P. Effect of Darapladib on Major Coronary Events After an Acute Coronary Syndrome. *Jama* **2014**, *312* (10), 1006.

(30) Tawakol, A.; Singh, P.; Rudd, J. H. F.; Soffer, J.; Cai, G.; Vucic, E.; Brannan, S. P.; Tarka, E. A.; Shaddinger, B. C.; Sarov-Blat, L.; Matthews, P.; Subramanian, S.; Farkouh, M.; Fayad, Z. A. Effect of Treatment for 12 Weeks with Rilapladib, a Lipoprotein-Associated Phospholipase A2 Inhibitor, on Arterial Inflammation as Assessed with 18F-Fluorodeoxyglucose-Positron Emission Tomography Imaging. *J. Am. Coll. Cardiol.* **2014**, *63* (1), 86–88.

(31) Wilensky, R. L.; Shi, Y.; Mohler, E. R.; Hamamdzic, D.; Burgert, M. E.; Li, J.; Postle, A.; Fenning, R. S.; Bollinger, J. G.; Hoffman, B. E.; Pelchovitz, D. J.; Yang, J.; Mirabile, R. C.; Webb, C. L.; Zhang, L.; Zhang, P.; Gelb, M. H.; Walker, M. C.; Zalewski, A.; Macphee, C. H. Inhibition of Lipoprotein-Associated Phospholipase A2 Reduces Complex Coronary Atherosclerotic Plaque Development. *Nat. Med.* **2008**, *14* (10), 1059–1066.

(32) Samanta, U.; Bahnson, B. J. Crystal Structure of Human Plasma Platelet-Activating Factor Acetylhydrolase: Structural Implication to Lipoprotein Binding and Catalysis. *J. Biol. Chem.* **2008**, *283* (46), 31617–31624.

(33) Liu, Q.; Chen, X.; Chen, W.; Yuan, X.; Su, H.; Shen, J.; Xu, Y. Structural and Thermodynamic Characterization of Protein–Ligand Interactions Formed between Lipoprotein-Associated Phospholipase A2 and Inhibitors. *J. Med. Chem.* **2016**, acs.jmedchem.6b00282.

(34) Young, R. J.; Green, D. V. S.; Luscombe, C. N.; Hill, A. P. Getting Physical in Drug Discovery II: The Impact of Chromatographic Hydrophobicity Measurements and Aromaticity. *Drug Discov. Today* **2011**, *16* (17-18), 822–830.

(35) Andrews, M. D.; Bagal, S. K.; Gibson, K.; R.; Omoto, K.; Ryckmans, T.; Skerratt, S. E.; Stupple, P. A. Pyrrolo[2,3-D]pyrimidine Derivatives as Inhibitors of Tropomyosinrelated Kinases and Their Preparation and Use in the Treatment of Pain. WO2012137089, 2012.

(36) Bennett, B.; L.; Elsner, J.; Erdman, P.; Hilgraf, R.; Lebrun, L. A.; McCarrick, M. .; Moghaddam, M. F.; Nagy, M. A.; Norris, S.; Paisner, D. A.; Sloss, M. .; Romanow, W. J.; Satoh, Y.; Tikhe, J.; Yoon, W. H.; Delgrado, M. Preparation of Substituted Diaminocarboxamide and Diaminocarbonitrile Pyrimidines as JNK Pathway Inhibitors. WO2012145569, 2012.

(37) Hayashi, K. .; Watanabe, T.; Toyama, K.; Kamon, J.; Minami, M.; Uni, M.; Nasu, M. Preparation of Tricyclic Heterocyclic Compounds as JAK Inhibitors. WO2013024895, 2012.

(38) Costantino, G.; Maltoni, K.; Marinozzi, M.; Camaioni, E.; Prezeau, L.; Pin, J.-P.; Pellicciari, R. Synthesis and Biological Evaluation of 2-(3′-(1H-Tetrazol-5-yl)bicyclo[1.1.1]pent-1-Yl)glycine (S-TBPG), a Novel mGlu1 Receptor Antagonist. *Bioorg. Med. Chem.* **2001**, *9* (2), 221–227.

(39) Pellicciari, R.; Filosa, R.; Fulco, M. C.; Marinozzi, M.; Macchiarulo, A.; Novak, C.; Natalini, B.; Hermit, M. B.; Nielsen, S.; Sager, T. N.; Stensbøl, T. B.; Thomsen, C. Synthesis and Preliminary Biological Evaluation of 2'-substituted 2-(3'-carboxybicyclo[1.1.1]pentyl)glycine Derivatives as Group I Selective Metabotropic Glutamate Receptor Ligands. *ChemMedChem* **2006**, *1* (3), 358–365.

(40) Stepan, A. F.; Subramanyam, C.; Efremov, I. V; Dutra, J. K.; O'Sullivan, T. J.; DiRico, K. J.; McDonald, W. S.; Won, A.; Dorff, P. H.; Nolan, C. E.; Becker, S. L.; Pustilnik, L. R.; Riddell, D. R.; Kauffman, G. W.; Kormos, B. L.; Zhang, L.; Lu, Y.; Capetta, S. H.; Green, M. E.; Karki, K.; Sibley, E.; Atchison, K. P.; Hallgren, A. J.; Oborski, C. E.; Robshaw, A. E.; Sneed, B.; O'Donnell, C. J. Application of the bicyclo[1.1.1]pentane Motif as a Nonclassical Phenyl Ring Bioisostere in the Design of a Potent and Orally Active γ-Secretase Inhibitor. *J. Med. Chem.* **2012**, *55* (7), 3414–3424.

(41) Belzner, J.; Bunz, U.; Semmler, K.; Szeimies, G.; Opitz, K.; Schlüter, A.-D. Concerning the Synthesis of [1.1.1]Propellane. *Chem. Ber.* **1989**, *122* (2), 397–398.

(42) Applequist, D. E.; Renken, T. L.; Wheeler, J. W. Polar Substituent Effects in 1,3-Disubstituted bicyclo[1.1.1]pentanes. *J. Org. Chem.* **1982**, *47* (25), 4985–4995.

(43) Kaszynski, P.; Michl, J. A Practical Photochemical Synthesis of bicyclo[1.1.1]pentane-1,3-Dicarboxylic Acid. *J. Org. Chem.* **1988**, *53* (19), 4593–4594.

(44) Hall, H. K.; Smith, C. D.; Blanchard, E. P.; Cherkofsky, S. C.; Sieja, J. B. Synthesis and Polymerization of Bridgehead-Substituted Bicyclobutanes. *J. Am. Chem. Soc.* **1971**, *93* (1), 121–130.

(45) Chatgilialoglu, C.; Griller, D.; Lesage, M. Tris(trimethylsilyl)silane. A New Reducing Agent. *J. Org. Chem.* **1988**, *53* (15), 3641–3642.

(46) Cheng, C.; Brookhart, M. Iridium-Catalyzed Reduction of Secondary Amides to Secondary Amines and Imines by Diethylsilane. *J. Am. Chem. Soc.* **2012**, *134* (28), 11304–11307.

(47) Lee, M. Patent. WO2013/30374 A1, 2013.

(48) Method and Statistics Provided in Supplementary Information.

(49) Darapladib Permeability Obtained at pH 7.05 and Analogue 5 Permeability Obtained at pH 7.4.

(50) Nicolaou, K. C.; Vourloumis, D.; Totokotsopoulos, S.; Papakyriakou, A.; Karsunky, H.; Fernando, H.; Gavrilyuk, J.; Webb, D.; Stepan, A. F. Synthesis and Biopharmaceutical Evaluation of Imatinib Analogues Featuring Unusual Structural Motifs. *ChemMedChem* **2016**, *11*, 31-37.

(51) Lovering, F.; Bikker, J.; Humblet, C. Escape From Flatland: Increasing Saturation as and Approach to Improving Clinical Success. *J. Med. Chem.* **2009**, *52*, 6752-6756.

(52) Shaddinger, B. C.; Xu, Y.; Roger, J. H.; Macphee, C. H.; Handel, M.; Baidoo, C. A.; Magee, M.; Lepore, J. J.; Sprecher, D. L. Platelet Aggregation Unchanged by Lipoprotein-associated Phospholipase A_2 Inhibition: Results from an In Vitro Study and Two Randomized Phase I Trials. *PLoS One*, **2014**, *9*, e83094.

Supporting Information

General experimental

Solvents and reagents. Unless otherwise stated, all reactions were carried out under an atmosphere of nitrogen in heat- or oven-dried glassware and using anhydrous solvent. Solvents and reagents were purchased from commercial suppliers and used as received. Reactions were monitored by thin layer chromatography (TLC) or liquid chromatographymass spectroscopy (LCMS). Heating was conducted using hotplates with DrySyn adaptors.

Chromatography. Thin layer chromatography (TLC) was carried out using plastic-backed 50 precoated silica plates (particle size 0.2 mm). Spots were visualised by ultraviolet (UV) light (λ_{max} = 254 nm or 365 nm) and then stained with potassium permanganate solution followed by gentle heating. Flash column chromatography was carried out using the Teledyne ISCO CombiFlash® Rf+ apparatus with RediSep® or GraceResolv™ silica cartridges.

Liquid chromatography mass spectrometry. LCMS analysis carried out using system 1 described below unless otherwise stated as using system 2.

System 1

LCMS analysis was carried out on an H_2Os Acquity UPLC instrument equipped with a BEH column (50 mm x 2.1 mm, 1.7 μm packing diameter) and H_2Os micromass ZQ MS using alternate-scan positive and negative electrospray. Analytes were detected as a summed UV wavelength of 210 – 350 nm. Three liquid phase methods were used:

Method A - Formic – 40 °C, 1 mL/min flow rate. Gradient elution with the mobile phases as (A) H_2O containing 0.1% volume/volume (v/v) formic acid and (B) acetonitrile containing 0.1% (v/v) formic acid. Gradient conditions were initially 1% B, increasing linearly to 97% B over 1.5 min, remaining at 97% B for 0.4 min then increasing to 100% B over 0.1 min.

Method B - High pH – 40 °C, 1 mL/min flow rate. Gradient elution with the mobile phases as (A) 10 mM aqueous ammonium bicarbonate solution, adjusted to pH 10 with 0.88 M aqueous ammonia and (B) acetonitrile. Gradient conditions were initially 1% B, increasing linearly to 97% B over 1.5 min, remaining at 97% B for 0.4 min then increasing to 100% B over 0.1 min.

Method C - TFA – 40 °C, 1 mL/min flow rate. Gradient elution with the mobile phases as (A) H_2O containing 0.1% volume/volume (v/v) TFA and (B) acetonitrile containing 0.1% (v/v) TFA. Gradient conditions were initially 1% B, increasing linearly to 97% B over 1.5 min, remaining at 97% B for 0.4 min then increasing to 100% B over 0.1 min.

System 2

LCMS analysis was carried out on an Agilent 1290 Infinity equipped with an acquity BEH column (50 mm x 2.1 mm, 1.7 µm packing diameter). Analytes were detected as a summed UV wavelength of 190 – 400 nm. Liquid phase method used:

Formic – 35 °C, 0.6 mL/min flow rate. Gradient elution with the mobile phases as (A) H_2O containing 0.1% volume/volume (v/v) formic acid and (B) acetonitrile containing 0.1% (v/v) formic acid. Gradient conditions were initially 3% B for 0.4 min, increasing linearly to 98% B over 2.8 min, remaining at 98% B for 0.6 min then decreasing to 3% B over 0.4 min then remaining at 3% B for 0.3 min. .

Nuclear magnetic resonance (NMR) spectroscopy. Proton (^{1}H), carbon (^{13}C), and fluorine (^{19}F) spectra were recorded in deuterated solvents at ambient temperature (unless otherwise stated) using standard pulse methods on any of the following spectrometers and signal frequencies: Bruker AV-400 (^{1}H = 400 MHz, ^{13}C = 101 MHz, ^{19}F = 376 MHz) and Bruker AV-600 (^{1}H = 600 MHz, ^{13}C = 150 MHz). Chemical shifts are reported in ppm and are referenced to tetramethylsilane (TMS) or the following solvent peaks: $CDCl_3$ (^{1}H =

7.27 ppm, ^{13}C = 77.0 ppm), DMSO-d_6 (^{1}H = 2.50 ppm, ^{13}C = 39.5 ppm), and MeOH-d_4 (^{1}H = 3.31 ppm, ^{13}C = 49.15 ppm). Peak assignments were made on the basis of chemical shifts, integrations, and coupling constants, using COSY, DEPT, and HSQC where appropriate. Coupling constants are quoted to the nearest 0.1 Hz and multiplicities are described as singlet (s), doublet (d), triplet (t), quartet (q), quintet (quin), sextet (sxt), septet (sept), br. (broad) and multiplet (m).

Infrared (IR) spectroscopy. Infrared spectra were recorded using a Perkin Elmer Spectrum 1 machine. Absorption maxima (ν_{max}) are reported in wavenumbers (cm^{-1}) and are described as strong (s), medium (m), weak (w) and broad (br).

High-resolution mass spectrometry (HRMS). High-resolution mass spectra were recorded on a Micromass Q-Tof Ultima hybrid quadrupole time-of-flight mass spectrometer, with analytes separated on an Agilent 1100 Liquid Chromatography equipped with a Phenomenex Luna C18 (2) reversed phase column (100 mm x 2.1 mm, 3 µm packing diameter). LC conditions were 0.5 mL/min flow rate, 35 ºC, injection volume 2–5 µL. Gradient elution with (A) H_2O containing 0.1% (v/v) formic acid and (B) acetonitrile containing 0.1% (v/v) formic acid. Gradient conditions were initially 5% B, increasing linearly to 100% B over 6 min, remaining at 100% B for 2.5 min then decreasing linearly to 5% B over 1 min followed by an equilibration period of 2.5 min prior to the next injection. Mass to charge ratios (*m/z*) are reported in Daltons.

Melting points. Melting points were recorded on a Stuart SMP10 melting point apparatus.

Mass directed auto preparation (MDAP). Mass-directed automated purification was carried out using an H_2Os ZQ MS using alternate-scan positive and negative electrospray and a summed UV wavelength of 210–350 nm. Two liquid phase methods were used:

Formic – Sunfire C18 column (100 mm x 19 mm, 5 µm packing diameter, 20 mL/min flow rate) or Sunfire C18 column (150 mm x 30 mm, 5 µm packing diameter, 40 mL/min flow rate). Gradient elution at ambient temperature with the mobile phases as (A) H_2O containing 0.1% volume/volume (v/v) formic acid and (B) acetonitrile containing 0.1% (v/v) formic acid.

High pH – Xbridge C18 column (100 mm x 19 mm, 5 µm packing diameter, 20 mL/min flow rate) or Xbridge C18 column (150 mm x 30 mm, 5 µm packing diameter, 40 mL/min flow rate). Gradient elution at ambient temperature with the mobile phases as (A) 10 mM aqueous ammonium bicarbonate solution, adjusted to pH 10 with 0.88 M aqueous ammonia and (B) acetonitrile.

TFA – Sunfire C18 column (100 mm x 19 mm, 5 µm packing diameter, 20 mL/min flow rate) or Sunfire C18 column (150 mm x 30 mm, 5 µm packing diameter, 40 mL/min flow rate). Gradient elution at ambient temperature with the mobile phases as (A) H_2O containing 0.1% volume/volume (v/v) TFA and (B) acetonitrile containing 0.1% (v/v) TFA.

The elution gradients used were at a flow rate of 40 mL/min over 10 or 20 min:

Gradient A	5-30% B
Gradient B	15-55% B
Gradient C	30-85% B
Gradient D	50-99% B
Gradient E	80-99% B

X-ray Crystallography.

- PDB file for compound **5** bound to $LpPLA_2$ available for immediate release upon publication.

Experimental

3-Hydroxy-3-(4-(trifluoromethyl)phenyl)cyclobutanecarboxylic acid – 7

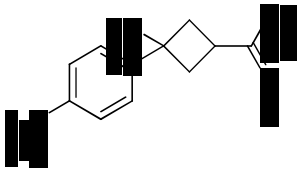

To 1-bromo-4-(trifluoromethyl)benzene (197 g, 876 mmol) in THF (1000 mL) was added nbutyllithium (2.5M in hexanes) (500 mL, 1250 mmol) at −78 ºC. The reaction was stirred for 2 h before 3-oxocyclobutanecarboxylic acid (50 g, 438 mmol) in THF (250 mL) was added dropwise at −78 ºC. The reaction was allowed to warm to ambient temperature and was stirred for 16 h. The reaction mixture was quenched with saturated NH_4Cl solution (200 mL) and basified with 2M NaOH solution (500 mL) and washed with ethyl acetate (700 mL). The layers were separated and the aqueous layer was acidified with 2M HCl solution (1000 mL). The aqueous was extracted with ethyl acetate (1000 mL) which was then dried over Na_2SO_4 and evaporated under reduced pressure to afford 3-hydroxy-3-(4-

(trifluoromethyl)phenyl)cyclobutanecarboxylic acid (100 g, 339 mmol, 77%) as a pale brown solid.

M.p. 113 – 115 ºC; LCMS (System 2, ESI) R_t = 2.21 $[M-H]^-$ = 259.1, 88% purity; ^{1}H NMR (400 MHz, DMSO-d_6) δ = 12.45 – 11.90 (br. s., 1H), 7.77 – 7.68 (m, 4H), 2.85 – 2.74 (m, 1H), 2.67 – 2.53 (m, 4H) 1.92 (s, 1H); ^{13}C NMR (101 MHz, DMSO-d_6) δ = 175.7, 151.6,

127.3 (q, $^2J_{C-F}$ = 31.5 Hz), 125.7, 124.9 (q, $^3J_{C-F}$ = 3.6 Hz), 124.3 (q, $^1J_{C-F}$ = 271.4 Hz), 70.8, 40.9, 28.5; ^{19}F NMR (376 MHz, DMSO-d_6) δ = −61.3 (s, 3F); ν_{max}/cm^{-1} (thin film) 3208 (br), 2957, 1701, 1683.

3-Chloro-3-(4-(trifluoromethyl)phenyl)cyclobutanecarboxylic acid 8

To 3-hydroxy-3-(4-(trifluoromethyl)phenyl)cyclobutanecarboxylic acid (16.18 g, 62.2 mmol) in toluene (300 mL) was added conc. HCl (50 mL, 617 mmol) at ambient temperature and the reaction was sonicated for 7 h. The layers were separated and the aqueous layer was extracted with toluene (2 × 50 mL). The organics were combined and washed with water (2 × 50 mL) and brine (2 × 50 mL). The organics were filtered through a hydrophobic frit and evaporated under reduced pressure to give 3-chloro-3-(4-(trifluoromethyl)phenyl)cyclobutanecarboxylic acid (13.1 g, 46.9 mmol, 75%) as a white solid. The isomers can be separated *via* the following procedure**.** The mixture was triturated with hexane and filtered to collect the solid washing with hexane. The solid was dried to afford *cis*-3-chloro-3-(4-

(trifluoromethyl)phenyl)cyclobutanecarboxylic acid as an off-white solid. The filtrate was evaporated under reduced pressure to afford *trans*-3-chloro-3-(4-

(trifluoromethyl)phenyl)cyclobutanecarboxylic acid as an off-white solid. ***cis*-3-Chloro-3-(4-(trifluoromethyl)phenyl)cyclobutanecarboxylic acid – 8**

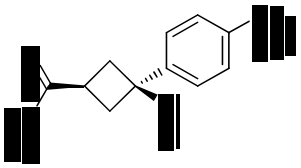

M.p. 172 – 174 ºC; LCMS (Method B, UV, ESI) R_t = 0.72 $[M-H]^-$ = No mass ion peak, 100% purity; ^{1}H NMR (400 MHz, DMSO-d_6) δ = 12.50 (br. s., 1H), 7.88 – 7.74 (m, 4H), 3.34 – 3.21 (m, 2H), 3.08 – 2.97 (m, 2H), 2.92 – 2.80 (m, 1H); ^{13}C NMR (101 MHz, DMSOd_6) δ = 174.5, 147.8, 128.5 (q, $^2J_{C-F}$ = 31.5 Hz), 127.0, 125.2 (q, $^3J_{C-F}$ = 3.6 Hz), 124.0 (q, $^1J_{CF}$ = 272.2 Hz), 65.0, 41.9, 31.1; ^{19}F NMR (376 MHz, $CDCl_3$) δ = −62.8 (s, 3F); v_{max}/cm^{-1} (thin film) 2989, 1687; HRMS: Calculated for $C_{12}H_9ClF_3O_2$ 277.0249 Found $[M-H]^-$:

277.0251 (0.8 ppm). ***trans*-3-Chloro-3-(4-(trifluoromethyl)phenyl)cyclobutanecarboxylic acid – 8**

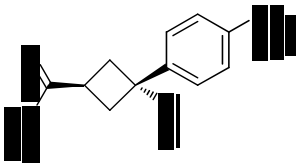

M.p. 114 – 116 ºC; LCMS (Method B, UV, ESI) R_t = 0.71 $[M-H]^-$ = 277.4, 81% purity; ^{1}H NMR (400 MHz, $CDCl_3$) δ = 7.66 (d, J = 8.3 Hz, 2H), 7.49 (d, J = 8.1 Hz, 2H), 3.78 (quin,
J = 8.8 Hz, 1H), 3.15 – 3.02 (m, 4H); ^{13}C NMR (101 MHz, $CDCl_3$) δ = 179.6, 148.3 130.3 (q,

$^2J_{C-F}$ = 32.8 Hz), 125.7 (q, $^3J_{C-F}$ = 4.0 Hz), 125.5, 123.8 (q, $^1J_{C-F}$ = 272.3 Hz), 66.8, 41.5,

32.5; ^{19}F NMR (376 MHz, $CDCl_3$) δ = −63.2 (s, 3F); v_{max}/cm^{-1} (thin film) 2947, 1705;

HRMS: Calculated for $C_{12}H_{11}ClF_3O_2$ 279.0394 Found $[M+H]^+$: 279.0401 (2.3 ppm).

Methyl 3-chloro-3-(4-(trifluoromethyl)phenyl)cyclobutanecarboxylate – 9

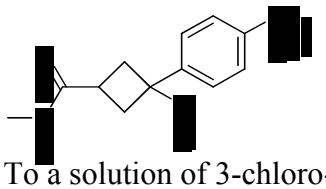

To a solution of 3-chloro-3-(4-trifluoromethyl)phenyl)cyclobutanecarboxylic acid (10 g, 35.9 mmol) and HCl (4M in 1,4-dioxane) (45 mL, 180 mmol) in 1,4-dioxane (100 mL) stirred under nitrogen at ambient temperature was added methanol (100 mL, 2472 mmol). The reaction mixture was stirred at ambient temperature for 3 h. Saturated aq. $NaHCO_3$ (20 mL) and ethyl acetate (20 mL) were added and the layers were separated. The aqueous layer was extracted with ethyl acetate (3 × 20 mL) and the combined organics were evaporated under reduced pressure to give methyl 3-chloro-3-(4-trifluoromethyl)phenyl)cyclobutanecarboxylate (10.5 g, 35.9 mmol, quant.) as a pale yellow liquid.

Analogously, the isomers of **9** could be produced using isomerically pure starting materials.

Data provided of individual isomers:

***cis*-Methyl 3-chloro-3-(4-(trifluoromethyl)phenyl)cyclobutanecarboxylate – 9**

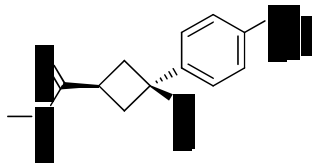

M.p. 52 – 54 ºC; LCMS (Method B, UV, ESI) R_t = 1.29 $[M-H]^-$ = No mass ion peak, 100% purity; ^{1}H NMR (400 MHz, $CDCl_3$) δ = 7.71 – 7.63 (m, 4H), 3.77 (s, 3H), 3.28 – 3.16 (m, 4H), 2.95 – 2.84 (m, 1H); ^{13}C NMR (101 MHz, $CDCl_3$) δ = 173.6, 147.3, 130.3 (q, $^2J_{C\text{-}F}$ = 33.1 Hz), 126.3, 125.7 (q, $^3J_{C\text{-}F}$ = 3.6 Hz), 123.8 (q, $^1J_{C\text{-}F}$ = 272.2 Hz), 63.4, 52.2, 42.4, 31.8;

^{19}F NMR (376 MHz, $CDCl_3$) δ = −62.7 (s, 3F); ν_{max}/cm^{-1} (thin film) 2957, 1739.

trans-Methyl 3-chloro-3-(4-(trifluoromethyl)phenyl)cyclobutanecarboxylate – 9

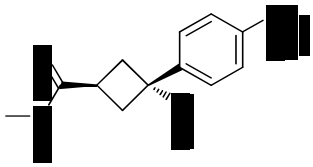

LCMS (Method B, UV, ESI) R_t = 1.31 $[M+H]^+$ = No mass ion peak, 80% purity; ^{1}H NMR (400 MHz, $CDCl_3$) δ = 7.66 (d, J = 8.3 Hz, 2H), 7.50 (d, J = 8.3 Hz, 2H), 3.80 – 3.67 (m, 4H), 3.14 – 2.98 (m, 4H); ^{13}C NMR (101 MHz, $CDCl_3$) δ = 174.1, 148.5, 130.2 (q, $^2J_{C\text{-}F}$ =

32.8 Hz), 125.7 (q, $^3J_{C\text{-}F}$ = 4.0 Hz), 125.5, 123.8 (q, $^1J_{C\text{-}F}$ = 272.3 Hz), 67.1, 52.0, 41.6, 32.6;

^{19}F NMR (376 MHz, $CDCl_3$) δ = −63.2 (s, 3F); v_{max}/cm^{-1} (thin film) 2955, 1733; HRMS: Calculated for $C_{13}H_{13}ClF_3O_2$ 293.0551 Found $[M+H]^+$: 293.0551 (0.1 ppm).

Methyl 3-(4-(trifluoromethyl)phenyl)bicyclo[1.1.0]butane-1-carboxylate – 10

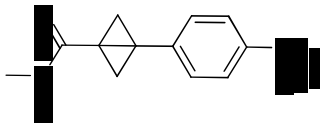

To solid sodium hydride (60% dispersion in oil) (8.2 g, 205 mmol) in THF (250 mL) stirred under nitrogen at ambient temperature was added a solution of *cis*-methyl 3-chloro-3-(4(trifluoromethyl)phenyl)cyclobutanecarboxylate (50 g, 171 mmol) in THF (250 mL) portionwise. The reaction mixture was stirred at ambient temperature for 3 h. To the reaction mixture was added $NH_4Cl_{(aq)}$ (100 mL) and ethyl acetate (350 mL) then water (100 mL). The layers were separated and the aqueous layer was extracted with ethyl acetate (3 x 50 mL). The organics were combined and dried through a hydrophobic frit. The solvent was

evaporated under reduced pressure to give methyl 3-(4-(trifluoromethyl)phenyl)bicyclo[1.1.0]butane-1-carboxylate (43.1 g, 168 mmol, 98%) as a yellow solid.

M.p. 102 – 104, LCMS (Method B, UV, ESI) R_t = 1.21 $[M+H]^+$ = No mass ion peak, 100% purity; ^{1}H NMR (400 MHz, $CDCl_3$) δ = 7.56 (d, J = 8.3 Hz, 2H), 7.39 (d, J = 8.1 Hz, 2H), 3.51 (s, 3H), 2.96 (t, J = 1.1 Hz, 2H), 1.67 (t, J = 1.1 Hz, 2H); ^{13}C NMR (101 MHz, $CDCl_3$) δ = 169.4, 138.3, 129.0 (q, $^2J_{C\text{-}F}$ = 33.1 Hz), 126.1, 125.4 (q, $^3J_{C\text{-}F}$ = 43.3 Hz), 124.1 (q, $^1J_{CF}$ = 272.1 Hz), 52.0, 36.0, 31.6, 24.4; ^{19}F NMR (376 MHz, $CDCl_3$) δ = −62.5 (s, 3F); v_{max}/cm^{-1} (thin film) 2956, 1708; HRMS: Calculated for $C_{13}H_{12}F_3O_2$ 257.0784 Found $[M+H]^+$: 257.0785 (0.5 ppm).

Methyl 2,2-dichloro-3-(4-(trifluoromethyl)phenyl)bicyclo[1.1.1]pentane-1-carboxylate – 11

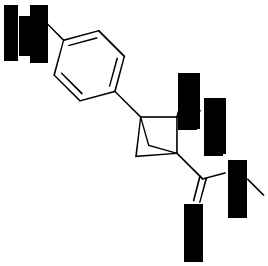

Methyl 3-(4-(trifluoromethyl)phenyl)bicyclo[1.1.0]butane-1-carboxylate (5 g, 19.51 mmol) was dissolved in diethylene glycol dimethyl ether (10 mL) and tetrachloroethylene (PCE) (30 mL) and the reaction mixture was heated to 120 ºC. Solid sodium 2,2,2-trichloroacetate (18.09 g, 98 mmol) was added portionwise over 30 min and the reaction was stirred at 140 ºC for an additional 30 min. Water (100 mL) and CH_2Cl_2 (100 mL) were added and the layers were separated. The organic layer was washed with brine (10 × 50 mL) and was then filtered through a hydrophobic frit. Added CH_2Cl_2 (100 mL) and this was washed with brine (5 × 50 mL) and then 5% $LiCl_{(aq)}$ (5 × 50 mL) to remove diethylene glycol dimethyl ether. The organic layer was filtered through a hydrophobic frit and the solvent was removed under reduced pressure to give the crude product. This was purified using column chromatography eluting with 0-20 cyclohexane:TBME. Collected fractions containing product were evaporated under reduced pressure to give methyl 2,2-dichloro-3-(4-

(trifluoromethyl)phenyl)bicyclo[1.1.1]pentane-1-carboxylate (2.5 g, 7.37 mmol, 38%) as a yellow oil.

LCMS (Method B, UV, ESI) R_t = 1.38 $[M-H]^-$ = No mass ion peak, 81% purity; ^{1}H NMR

(600 MHz, $CDCl_3$) δ = 7.66 (d, J = 8.1 Hz, 2H), 7.51 (d, J = 7.9 Hz, 2H), 3.85 (s, 3H), 3.14 (d, J = 1.3 Hz, 2H), 2.47 (d, J = 1.3 Hz, 2H); ^{13}C NMR (150 MHz, $CDCl_3$) δ = 165.4, 135.9

(q, $^4J_{C\text{-}F}$ = 1.4 Hz), 130.9 (q, $^2J_{C\text{-}F}$ = 32.6 Hz), 127.6, 125.5 (q, $^3J_{C\text{-}F}$ = 3.8 Hz), 123.9 (q, $^1J_{CF}$ = 272.3 Hz), 94.0, 57.0, 52.5, 52.4, 49.4; ^{19}F NMR (376 MHz, $CDCl_3$) δ = −63.2 (s, 3F); ν_{max}/cm^{-1} (thin film) 2957, 1737; HRMS: Calculated for $C_{14}H_{13}Cl_2F_3O_2$ 339.0161 Found $[M+H]^+$: 339.0169 (2.5 ppm).

Methyl 3-(4-(trifluoromethyl)phenyl)bicyclo[1.1.1]pentane-1-carboxylate – 12

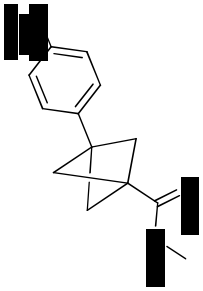

To azobis(cyclohexanecarbonitrile) (ACHN) (94 mg, 0.39 mmol) was added methyl 2,2dichloro-3-(4-(trifluoromethyl)phenyl)bicyclo[1.1.1]pentane-1-carboxylate (2.3 g, 6.78 mmol) in toluene (50 mL). Then tris(trimethylsilyl)silane (TTMSS) (11 mL, 38.9 mmol) was added. The reaction was heated under reflux for 3 h. ACHN (1.9 g, 7.77 mmol) was added portionwise over 4 days with continued heating under reflux. The solvent was removed under reduced pressure and the crude product was purified using column chromatography eluting with 0-20% cyclohexane:TBME. Fractions containing product were impure and these were purified using column chromatography eluting with 0-10% cyclohexane:TBME. Fractions containing product were evaporated under reduced pressure to give methyl 3-(4(trifluoromethyl)phenyl)bicyclo[1.1.1]pentane-1-carboxylate (1.36 g, 5.03 mmol, 74%) as a white solid.

M.p. 54 – 56 °C; LCMS (Method B, UV, ESI) R_t = 1.31 $[M+H]^+$ = No mass ion peak, 100% purity; ^{1}H NMR (400 MHz, $CDCl_3$) δ = 7.59 (d, J = 8.1 Hz, 2H), 7.34 (d, J = 7.8 Hz, 2H), 3.75 (s, 3H), 2.38 (s, 6H);^{13}C NMR (101 MHz, $CDCl_3$) δ = 170.3, 143.5 (q, $^4J_{C-F}$ = 1.5 Hz),

129.2 (q, $^2J_{C-F}$ = 32.3 Hz), 126.5, 125.2 (q, $^3J_{C-F}$ = 3.7 Hz), 124.2 (q, $^1J_{C-F}$ = 272.2 Hz),

53.4, 51.7, 41.5, 37.1; ^{19}F NMR (376 MHz, $CDCl_3$) δ = −62.5 (s, 3F); ν_{max}/cm^{-1} (thin film) 2982, 1737; HRMS: Calculated for $C_{14}H_{14}F_3O_2$ 271.0940 Found [M+H]+: 271.0944 (1.4 ppm). **3-(4-(Trifluoromethyl)phenyl)bicyclo[1.1.1]pentane-1-carboxylic acid – 13**

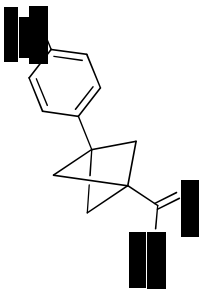

To methyl 3-(4-(trifluoromethyl)phenyl)bicyclo[1.1.1]pentane-1-carboxylate (1.3 g, 4.81 mmol) in 1,4-dioxane (10 mL) was added lithium hydroxide (9.62 mL, 9.62 mmol). This

was stirred at ambient temperature for 3h. To the reaction was added 2M $HCl_{(aq)}$ (5 mL) and ethyl acetate (30 mL). The layers were separated and the aqueous layer was extracted with ethyl acetate (3 x 10 mL). The organic layers were combined and evaporated under reduced pressure to give 3-(4-(trifluoromethyl)phenyl)bicyclo[1.1.1]pentane-1-carboxylic acid (1.17 g, 4.57 mmol, 95%) as a white solid.

M.p. 233 – 235 °C; LCMS (Method B, UV, ESI) R_t = 0.73 $[M-H]^-$ = 255.6, 98% purity; ^{1}H NMR (400 MHz, DMSO-d_6) δ = 12.60 – 12.27 (m, 1H), 7.68 (d, J = 8.1 Hz, 2H), 7.47 (d, J =
7.8 Hz, 2H), 2.28 (s, 6H); ^{13}C NMR (101 MHz, DMSO-d_6) δ = 170.9, 144.2, 127.5 (q, $^2J_{C-F}$ =

32.8 Hz), 126.9, 125.1 (q, $^3J_{C-F}$ = 3.7 Hz), 124.3 (q, $^1J_{C-F}$ = 272.2 Hz), 52.6, 40.6, 36.8;

^{19}F NMR (376 MHz, DMSO-d_6) δ = −60.9 (s, 3F); v_{max}/cm^{-1} (thin film) 2939, 1697;

HRMS:

Calculated for $C_{13}H_{12}F_3O_2$ 257.0784 Found [M+H]+: 257.0789 (2.0 ppm).

_N_-(2-(Diethylamino)ethyl)-3-(4-(trifluoromethyl)phenyl)bicyclo[1.1.1]pentane-1carboxamide – 15

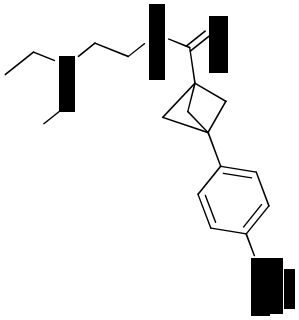

T3P (50% in ethyl acetate) (2.8 mL, 4.70 mmol), 3-(4-(trifluoromethyl)phenyl)bicyclo[1.1.1]pentane-1-carboxylic acid (800 mg, 3.12 mmol) and triethylamine (0.9 mL, 6.46 mmol) was stirred in ethyl acetate (10 mL) for 30 min. Then *N*1,*N*1-diethylethane-1,2-diamine (0.66 mL, 4.70 mmol) was added and the reaction mixture was stirred for 16 h. Water (15 mL) and CH_2Cl_2 (20 mL) were added and the layers separated. The aqueous was extracted with CH_2Cl_2 (3 x 5 mL) and the organics were combined and evaporated under reduced pressure to give *N*-(2-(diethylamino)ethyl)-3-(4(trifluoromethyl)phenyl)bicyclo[1.1.1]pentane-1-carboxamide (1.10 g, 3.10 mmol, 99%) as a orange solid.

M.p. 81 – 83 °C; LCMS (Method B, UV, ESI) R_t = 1.17 $[M+H]^+$ = 355.5, 94% purity; ^{1}H NMR (400 MHz, $CDCl_3$) δ = 7.58 (d, J = 7.8 Hz, 2H), 7.34 (d, J = 8.1 Hz, 2H), 6.48 – 6.36 (m, 1H), 3.39 – 3.27 (m, 2H), 2.61 – 2.52 (m, 6H), 2.32 (s, 6H), 1.05 (t, J = 7.1 Hz, 6H); ^{13}C NMR (101 MHz, $CDCl_3$) δ = 169.7, 143.7, 129.2 (q, $^2J_{C\text{-}F}$ = 33.0 Hz), 126.5, 125.2 (q, $^3J_{C\text{-}F}$ = 3.7 Hz), 124.1 (q, $^1J_{C\text{-}F}$ = 272.2 Hz), 52.8, 51.3, 47.0, 40.5, 38.8, 36.7, 12.1; ^{19}F NMR (376 MHz, $CDCl_3$) δ = −62.5 (s, 3F); v_{max}/cm^{-1} (thin film) 3320 (br) 2975, 1642; HRMS:
Calculated for $C_{19}H_{26}F_3N_2O$ 355.1992 Found [M+H]+: 355.2000 (2.2 ppm).

_N_1,_N_1-Diethyl-_N_2-((3-(4-(trifluoromethyl)phenyl)bicyclo[1.1.1]pentan-1yl)methyl)ethane-1,2-diamine – 16

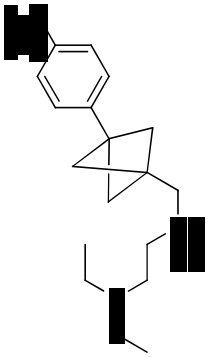

To *N*-(2-(diethylamino)ethyl)-3-(4-(trifluoromethyl)phenyl)bicyclo[1.1.1]pentane-1carboxamide (978 mg, 2.76 mmol) in THF (30 mL) was added $LiAlH_4$ (2.3 M in 2-MeTHF) (2.4 mL, 5.52 mmol) at ambient temperature and the reaction mixture was stirred for 16 h. The reaction was quenched by the addition of wet THF (20 mL) initially dropwise then portionwise. Water (20 mL) was then added portionwise, followed by 2M HCl (50 mL) and ethyl acetate (50 mL). The layers were separated and the organic layer was extracted with 2M HCl (3 x 10 mL). The aqueous layers were combined and basified with 2M NaOH (100 mL) then extracted with CH_2Cl_2 (10 x 50 mL). The organics were combined and filtered through a hydrophobic frit and evaporated under reduced pressure to give the crude *N*1,*N*1-diethyl-*N*2-

((3-(4-(trifluoromethyl)phenyl)bicyclo[1.1.1]pentan-1-yl)methyl)ethane-1,2-diamine

(527 mg, 1.55 mmol, 56%). LCMS showed 87% product and this was taken on as is to the next step without further purification.

LCMS (Method B, UV, ESI) R_t = 1.29 $[M+H]^+$ = 340.6, 87% purity.

_N_-(2-(Diethylamino)ethyl)-2-(2-((4-fluorobenzyl)thio)-4-oxo-4,5,6,7-tetrahydro-1_H_cyclopenta[d]pyrimidin-1-yl)-_N_-((3-(4-(trifluoromethyl)phenyl)bicyclo[1.1.1]pentan-1yl)methyl)acetamide, Formic acid salt – 5

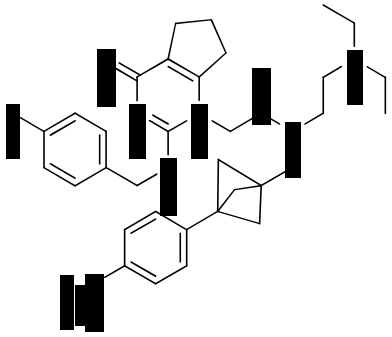

2-(2-((4-Fluorobenzyl)thio)-4-oxo-4,5,6,7-tetrahydro-1*H*-cyclopenta[d]pyrimidin-1-yl)acetic acid (634 mg, 1.90 mmol), triethylamine (0.350 mL, 2.509 mmol) and T3P (50% in ethyl acetate) (1.1 mL, 1.85 mmol) were stirred in CH_2Cl_2 (5 mL) for 30 min. Then *N*1,*N*1-diethyl*N*2-((3-(4-(trifluoromethyl)phenyl)bicyclo[1.1.1]pentan-1-yl)methyl)ethane-1,2-diamine (427 mg, 1.25 mmol) in CH_2Cl_2 (5 mL) was added and this was stirred for 16 h. To the reaction mixture was added 2M $NaOH_{(aq)}$ (20 mL), water (20 mL) and CH_2Cl_2 (40 mL). The layers were separated and the aqueous layer was extracted with CH_2Cl_2 (10 x 15 mL). The organics were combined and evaporated under reduced pressure. The crude product was purified by HpH MDAP, Method D to give product contaminated with formic acid and HpH modifier. The product was purified using HpH MDAP (Method D) and the solvent was removed under reduced pressure to give *N*-(2-(diethylamino)ethyl)-2-(2-((4-fluorobenzyl)thio)-4-oxo-

4,5,6,7-tetrahydro-1*H*-cyclopenta[d]pyrimidin-1-yl)-*N*-((3-(4-

(trifluoromethyl)phenyl)bicyclo[1.1.1]pentan-1-yl)methyl)acetamide, Formic acid salt (526 mg, 0.75 mmol, 60%) as a yellow solid.

M.p. 88 – 90 °C; LCMS (Method B, UV, ESI) R_t = 1.44 $[M+H]^+$ = 657.7, 100% purity; ^1H

NMR (400 MHz, DMSO-d_6, 373 K) δ = 8.14 (s, 1H), 7.64 (d, *J* = 8.1 Hz, 2H), 7.47 – 7.41 (m, 2H), 7.41 – 7.36 (m, 2H), 7.03 (br. s., 2H), 5.00 – 4.80 (m, 2H), 4.46 (s, 2H), 3.57 (br. s., 2H), 3.40 (t, *J* = 6.5 Hz, 2H), 2.79 (t, *J* = 7.6 Hz, 2H), 2.67 – 2.52 (m, 8H), 2.14 – 1.95 (m,
8H), 0.98 (t, *J* = 7.1 Hz, 6H);^{13}C NMR (101 MHz, $CDCl_3$) δ = 167.6, 167.1, 164.9, 163.5,

160.7, 156.0, 155.6, 144.2, 143.2, 131.6, 131.1, 130.1, 126.3, 125.3, 125.2, 121.4, 121.2, 115.7, 115.4, 115.4, 52.4, 52.2, 51.4, 49.7, 49.6, 48.8, 47.8, 47.4, 47.1, 46.4, 43.8, 42.3, 41.8,
37.2, 37.0, 36.3, 36.3, 32.0, 31.9, 28.3, 20.8, 20.7, 11.6, 9.8; ^{19}F NMR (376 MHz, $CDCl_3$) δ = −62.5 (s, 3F), -114.2 (s, 1F); v_{max}/cm^{-1} (thin film) 2969, 1618; HRMS: Calculated for $C_{35}H_{41}F_4N_4O_2S$ 657.2881 Found [M+H]+: 657.2883 (0.4 ppm).

N-(2-(diethylamino)ethyl)-2-(2-((4-fluorobenzyl)thio)-4-oxo-4,5,6,7-tetrahydro-1*H*cyclopenta[d]pyrimidin-1-yl)-*N*-((3-(4-(trifluoromethyl)phenyl)bicyclo[1.1.1]pentan-1yl)methyl)acetamide, Formic acid salt (100 mg,) was dissolved in MeOH (2 mL) then passed through an SAX cartridge eluting with MeOH (3 CVs). This collected fractions were evaporated under reduced pressure to give *N*-(2-(diethylamino)ethyl)-2-(2-((4fluorobenzyl)thio)-4-oxo-4,5,6,7-tetrahydro-1*H*-cyclopenta[d]pyrimidin-1-yl)-*N*-((3-(4(trifluoromethyl)phenyl)bicyclo[1.1.1]pentan-1-yl)methyl)acetamide (87 mg, 0.132 mmol) as a yellow solid.

LCMS (Method B, UV, ESI) R_t = 1.45 $[M+H]^+$ = 657.3, 100% purity; ^{1}H NMR (400 MHz, $CDCl_3$) δ = 7.58 (dd, *J* = 3.5, 7.9 Hz, 2H), 7.40 – 7.29 (m, 2H), 7.25 (t, *J* = 8.1 Hz, 2H), 7.02 – 6.94 (m, 1H), 6.89 – 6.81 (m, 1H), 4.92 – 4.64 (m, 2H), 4.53 (d, *J* = 4.2 Hz, 2H), 3.63 – 3.52 (m, 3H), 3.40 – 3.31 (m, 1H), 2.92 – 2.75 (m, 6H), 2.62 – 2.52 (m, 3H), 2.17 – 1.94 (m, 9H), 1.19 – 1.06 (m, 3H), 1.02 (t, *J* = 7.2 Hz, 3H).

N-(1-(2-Methoxyethyl)piperidin-4-yl)-3-(4trifluoromethyl)phenyl)bicyclo[1.1.1]pentane-1-carboxamide – 19

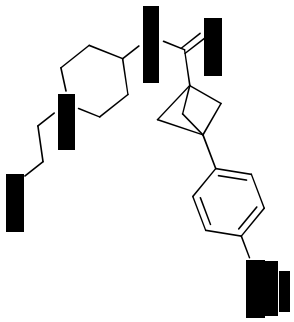

T3P (50% in DMF) (0.68 mL, 1.17 mmol), 3-(4-(trifluoromethyl)phenyl)bicyclo[1.1.1]pentane-1-carboxylic acid (200 mg, 0.781 mmol) and Et_3N (0.22 mL, 1.58 mmol) were stirred in CH_2Cl_2 (1 mL) for 20 min. Then 1-(2methoxyethyl)piperidin-4-amine (0.194 mL, 1.17 mmol) was added and the reaction mixture was stirred for 3 h. Water (2 mL) and CH_2Cl_2 (5 mL) were added and the layers separated. The organic layer was washed with 5% aq. LiCl (2 x 2 mL). The combined aqueous layers were extracted with DCM (2 x 3 mL). The organics were combined and filtered through a hydrophobic frit. The solvent was removed under reduced pressure to give *N*-(1-(2methoxyethyl)piperidin-4-yl)-3-(4-(trifluoromethyl)phenyl)bicyclo[1.1.1]pentane-1carboxamide (228 mg, 0.58 mmol, 74% yield) as an off white solid.

M.p. 185 – 187 °C; LCMS (Method B, UV, ESI) R_t = 1.07 $[M+H]^+$ = 397.2, 100% purity; ^{1}H

NMR (400 MHz, DMSO-d_6) δ = 7.68 (d, *J* = 8.1 Hz, 2H), 7.62 (d, *J* = 7.8 Hz, 1H), 7.45 (d, *J* = 8.1 Hz, 2H), 3.58 - 3.47 (m, 1H), 3.41 (t, *J* = 6.0 Hz, 2H), 3.23 (s, 3H), 2.84 (m, 2H), 2.45 (t, *J* = 6.0 Hz, 2H), 2.22 (s, 6H), 2.04 – 1.94 (m, 2H), 1.70 – 1.61 (m, 2H), 1.53

– 1.40 (m, 2H); ^{13}C NMR (101 MHz, DMSO-d$_6$) δ = 168.2, 144.7, 127.3 (q, $^{2}J_{C\text{-}F}$ = 31.5 Hz), 126.8, 125.1 (q, $^{3}J_{C\text{-}F}$ = 3.8 Hz), 124.3 (q, $^{1}J_{C\text{-}F}$ = 271.4 Hz), 70.1, 57.9, 57.0, 52.8, 52.3, 46.2, 38.3, 31.5 (1C concealed); ^{19}F NMR (376 MHz, $CDCl_3$) δ = −62.5 (s, 3F); ν_{max}/cm^{-1} (thin film) 3345, 2942, 1637; HRMS: Calculated for $C_{21}H_{28}F_3N_2O_2$ 397.2097 Found [M+H]+: 397.2096 (−0.4 ppm).

1-(2-Methoxyethyl)-*N*-((3-(4-(trifluoromethyl)phenyl)bicyclo[1.1.1]pentan-1yl)methyl)piperidin-4-amine, formic acid salt – 20

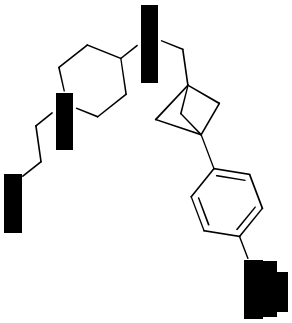

To $[Ir(COE)_2Cl]_2$ (48.4 mg, 0.054 mmol) was added diethylsilane (0.210 mL, 1.62 mmol) and CH_2Cl_2 (0.5 mL). To this was added *N*-(1-(2-methoxyethyl)piperidin-4-yl)-3-(4(trifluoromethyl)phenyl)bicyclo[1.1.1]pentane-1-carboxamide (107 mg, 0.27 mmol) in CH_2Cl_2 (1.5 mL). The reaction mixture was stirred for 20 h at ambient temperature. To the reaction mixture was added 4M HCl in 1,4-dioxane (3 mL), however no solid precipitation. 2M NaOH(aq) was added until alkaline pH achieved. CH_2Cl_2 (20 mL) was added and the layers were separated. The aqueous layer was extracted with CH_2Cl_2 (3 x 10 mL). The organic layers were combined and evaporated under reduced pressure to give a crude product. The crude product LCMS showed only desired product. NMR showed diethylsilane peaks. To the crude product was added CH_2Cl_2 (10 mL) and 2M HCl (10 mL) and the layers were separated. The organic layer was extracted with 2M HCl (3 x 5 mL). The aqueous layers were combined and 2M $NaOH_{(aq)}$ was added until alkaline pH. CH_2Cl_2 (30 mL) was added and the layers were separated. The aqueous layer was extracted with CH_2Cl_2 (6 x 20 mL) and the organics were combined and evaporated under reduced pressure to give a residue which was purified using HpH MDAP (Method C) to give 1-(2-methoxyethyl)-*N*-((3-(4-

(trifluoromethyl)phenyl)bicyclo[1.1.1]pentan-1-yl)methyl)piperidin-4-amine, formic acid salt (61 mg, 0.16 mmol, 59%) as a yellow solid.

M.p. 118 – 120 °C; LCMS (Method B, UV, ESI) R_t = 1.33 $[M+H]^+$ = 383.2, 100% purity; ^{1}H

NMR (400 MHz, $CDCl_3$) δ = 8.46 (s, 1H), 7.54 (d, *J* = 8.1 Hz, 2H), 7.31 – 7.27 (m, 2H), 5.23 (br. s., 2H), 3.61 (t, *J* = 5.1 Hz, 2H), 3.35 (s, 3H), 3.26 – 3.19 (m, 2H), 3.05 – 2.96 (m, 3H),

2.80 (t, J = 5.3 Hz, 2H), 2.47 – 2.37 (m, 2H), 2.17 – 2.10 (m, 8H), 1.95 – 1.82 (m, 2H); ^{13}C NMR (101 MHz, $CDCl_3$) δ = 167.5, 144.0, 128.9 (q, $^{2}J_{C\text{-}F}$ = 32.3 Hz), 126.4, 125.1 (q, $^{3}J_{C\text{-}F}$ = 3.6 Hz), 69.2, 58.8, 56.8, 53.6, 52.2, 51.6, 45.6, 42.0, 36.4, 28.3 (1C concealed); ^{19}F NMR (376 MHz, $CDCl_3$) δ = −62.4 (s, 3F); v_{max}/cm^{-1} (thin film) 2782 (br), 1619, 1560; HRMS:

Calculated for $C_{21}H_{30}F_3N_2O$ 383.2305 Found $[M+H]^+$: 383.2307 (0.5 ppm).

2-(2-((2,3-Difluorobenzyl)thio)-4-oxoquinolin-1(4*H*)-yl)-*N*-(1-(2-methoxyethyl)piperidin4-yl)-*N*-((3-(4-(trifluoromethyl)phenyl)bicyclo[1.1.1]pentan-1-yl)methyl)acetamide – 22

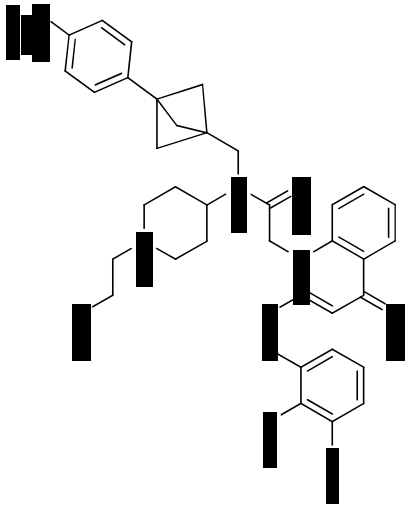

2-(2-((2,3-Difluorobenzyl)thio)-4-oxoquinolin-1(4*H*)-yl)acetic acid (28.3 mg, 0.078 mmol), Et_3N (0.015 mL, 0.11 mmol) and T3P (50% in DMF) (0.046 mL, 0.078 mmol) in CH_2Cl_2

(0.5 mL) was stirred for 15 min at ambient temperature. To the reaction mixture was added 1-

(2-methoxyethyl)-*N*-((3-(4-(trifluoromethyl)phenyl)bicyclo[1.1.1]pentan-1-

yl)methyl)piperidin-4-amine (20 mg, 0.052 mmol) in CH_2Cl_2 (0.500 mL) at ambient temperature stirred for 64 h. Water (1 mL) was added and the layers were separated. The aqueous layer was extracted with CH_2Cl_2 (3 x 1 mL). The organic layers were combined and evaporated under reduced pressure give a crude product. This was purified by HpH MDAP (Method D) to give 2-(2-((2,3-difluorobenzyl)thio)-4-oxoquinolin-1(4*H*)-yl)-*N*-(1-(2methoxyethyl)piperidin-4-yl)-*N*-((3-(4-(trifluoromethyl)phenyl)bicyclo[1.1.1]pentan-1yl)methyl)acetamide (20 mg, 0.028 mmol, 53% yield) as a yellow solid.

M.p. 57 – 59 °C; LCMS (Method B, UV, ESI) R_t = 1.36 $[M+H]^+$ = 726.2, 100% purity; ^{1}H NMR (400 MHz, DMSO-d_6, 373 K) δ = 8.18 (dd, J = 1.5, 8.1 Hz, 1H), 7.71 – 7.59 (m, 3H),

7.47 – 7.32 (m, 4H), 7.32 – 7.21 (m, 2H), 7.17 – 7.07 (m, 1H), 6.35 (s, 1H), 5.41 (br. s., 2H),

4.43 (s, 2H), 3.83 – 3.72 (m, 1H), 3.57 (br. s., 2H), 3.48 (t, J = 5.7 Hz, 2H), 3.28 (s, 3H), 3.00 (m, 2H), 2.56 (t, J = 5.6 Hz, 2H), 2.27 – 1.68 (m, 12H); ^{13}C NMR (101 MHz, $CDCl_3$) δ
= 176.5, 176.4, 166.5, 165.2, 152.1, 152.0, 142.3, 132.6, 132.4, 127.0, 126.9, 126.4, 126.3, 125.9, 125.3, 125.1, 124.5, 123.9, 117.5, 117.4, 115.3, 115.1, 113.3, 113.1, 77.2, 69.9, 69.1,

58.9, 58.9, 57.5, 56.9, 54.8, 53.2, 53.0, 52.9, 52.8, 52.2, 50.1, 49.9, 44.7, 43.4, 41.7, 41.0, 38.1, 37.8, 33.1, 33.0, 30.8, 28.3; ^{19}F NMR (376 MHz, DMSO-d_6) δ = −60.79 (s, 3F), −138.67 (m, 1F), −142.15 (m, 1F); ν_{max}/cm^{-1} (thin film) 3402 (br), 2964, 1652, 1617, 1593; HRMS: Calculated for $C_{39}H_{41}F_5N_3O_3S$ 726.2783 Found [M+H]+: 726.2796 (1.8 ppm).

X-ray crystallography

Materials and methods

Lp-PLA2 (residues 46-428 with a C-terminal His6 tag) was expressed, purified and crystallised essentially as previously described[1] though the purified protein was concentrated to 15mg/ml for crystallisation. To obtain the protein complex structure with **analogue-5**, a crystal was soaked in 30% PEG3350, 0.1 M HEPES pH 7.3, 0.2 M NaCl, 0.04% pluronic F68, 10 mM CHAPS and 2mM compound dissolved in DMSO for ~1 day.

The crystal was cryoprotected by briefly soaking in well buffer with 10% glycerol. A diffraction dataset was acquired at 100 K at the ESRF (station ID29) using a Pilatus 6M detector, and processed by the synchrotron autoprocessing suite (XDS_PARALLELPROC)[2] using XDS[3]. Data were merged using AIMLESS[4] within the CCP4 programming suite[5].

The crystal structure was solved by Fourier Synthesis using REFMAC[6] and a previously determined in-house Lp-PLA2 crystal structure as the starting model. Refinement was carried out with REFMAC and model building using COOT[7]. The final R_{factor} (and R_{free}) achieved were 16.2% (and 19.2%) and the structure was deposited into the PDB as entry 5LP1.

References

1
Woolford, A. J.-A. *et al.,* 2016. *J. Med. Chem.* **59**, 5356−5367.

2
Monaco S *et al.,* 2013. *J Appl Cryst.* **46**, 804-810.

3

Kabsch W. 2010. *Acta Cryst.* **D66**, 125-132.

[4] Evans, P.R. and Murshudov, G.N. 2013. *Acta Cryst.* **D69**, 1204-1214.

[5] Winn, M.D. *et al.,* 2010. *Acta Cryst.* **D67**, 235-242.

[6] Murshudov G.N. *et al.,* 1997. *Acta Cryst.* **D53**, 240-255.

[7] Emsley P and Cowtan K. 2004. *Acta Cryst.* **D60**, 2126-2132.

Table of Statistics

Lp-PLA2	Analogue 5
PARAMETER[a]	
DATA COLLECTION	
Space Group	C2
Cell Dimensions	
a,b,c (Å)	100.28,91.56,51.65
α, β, γ (°)	90.00,111.88, 90.00
Resolution (Å)	1.91 (1.98)
R_{merge}[b]	0.094 (0.624)
Average *I/σI*	7.8 (1.7)
Completeness (%)	98.7 (92.5)
Redundancy	3.4 (3.2)
No. Reflections	112961 (9618)
No. Unique Reflections	33162 (3045)
REFINEMENT	
Resolution (Å)	20.00-1.91
R_{work}/R_{free}	0.162/0.192
No. Reflections	31474
No. atoms	
Protein (chain A)	3040
Cmpd (L)	46
Water (W)	332
Cl^- (C)	2
B-factors [Å^2]	
Protein (chain A)	35.3
Cmpd (L)	37.0
Water (W)	47.4
Cl^- (C)	36.5
R.m.s deviations	
Bond lengths (Å)	0.007
Bond angles (°)	1.386

[a] Data for the highest resolution shell are given in parentheses.

[b] $R_{merge} = \Sigma|I_j - \langle I_j \rangle|/\Sigma\langle I_j \rangle$.